ISSN 2664-4169 (Print) & ISSN 2664-7923 (Online)
**South Asian Research Journal of Biology and Applied Biosciences**
*Abbreviated Key Title: South Asian Res J Bio Appl Biosci*

**| Volume-7 | Issue-3 | May-Jun -2025 |** **DOI: https://doi.org/10.36346/sarjbab.2025.v07i03.010**

**Original Research Article**

# Effect of SnO2+CNTs Deposition on SnS Thin Films: A Study of Optical and Structural Properties for Water Treatment by Photocatalytic Applications

Noor Amer Hakim[1*], Ameera O. Hussain Al-Janabi[2]

[1]Al-Qasim Green University, College of Environmental Science/ Department of Environmental Pollution, Iraq
[2]Al-Qasim Green University, College of Biotechnology, Department of Medical Biotechnology, Iraq

***Corresponding Author:** Noor Amer Hakim
Al-Qasim Green University, College of Environmental Science/ Department of Environmental pollution, Iraq

**Article History**
Received: 09.05.2025
Accepted: 14.06.2025
Published: 17.06.2025

**Abstract:** The (SnO2+CNTs/SnS) thin films deposited by the spray pyrolysis technique were used as photocatalytic application. The changes of structure, topography and optical characteristics upon the deposition of the upper layer were studied. The XRD revealed poly-crystalline mixed Orthorhombic and Zincblende phases and SnO 2 and C phases following the deposition of the upper layer. The FE-SEM images suggest the homogenous porous structure and the large differences in the surface morphology following the deposition of the upper layer. The UV-visible absorbance was enhanced, and the optical bandgap variation to tune to the peak of the solar spectrum. As the pH value rose beyond 8, the photocatalytic activity rose. The efficiency of degradation increased with deposition of the upper layer with the value rising to 95.84% after exposure to 120 min of solar radiation. These results lead to another approach to adjust the structural and optical quality of the SnS thin film by a simple method of nano-heterojunctions with an upper layer to apply to photocatalysis.

**Keywords:** SnS, $SnO_2$, CNT, Spray pyrolysis, Photocatalytic Application.

## 1. INTRODUCTION

Usually, semiconductors that soak up light and create reactive species that can degrade all kinds of environmental pollutants [1]. The most extensively examined and used photocatalyst is TiO2 [2]. The interest of many recent studies is to find alternatives that are applied in the photoanalysis technology [3, 4]. Stannous sulfide (SnS) is a chalcogenide semiconductor containing an almost optimal band gap with regard to solar absorbers in photovoltaic applications [5]. SnS is a p-type semiconductor that is favored by many applications because of its inexpensive price and non-toxicity [6]. Also, SnS thin films have been utilized in numerous researchers in the area of photocatalytic technology [7], including hydrogen production [8], and the destruction of organic contaminants, including dyes, in wastewater [9]. Deposits by chemical spray pyrolysis (CSP) are largely utilized in thin film deposition as an easy application method e.g. sensors, photocatalysis, etc. It falls in the category of chemical deposition techniques [10]. Among the various benefits of using this process against other deposition processes are; it is cost effective, it is easily doped, the thickness can be controlled and it deposits to a large area [11]. Dye pollution and in particular industrial processes like textile industries are very hazardous to the environment and to health. It is normally discharged into the waters, polluting drinking water sources. This has dire effects on aquatic life such as killing of fish and other aquatic life. Photocatalysis process is founded on the irradiation of a semiconductor with photons of energy (h) equal to or higher than the energy band gap (Eg) of the semiconductor, causes the translation of the electron in the valence band (V.B) to the conduction band (C.B) and therefore forming an electron-hole pair which participate in photocatalytic reactions [12, 13]. In this work we have tried to improve the photocatalytic activity of the SnS thin film prepared by the easy spray pyrolysis method. The changes in the structural, surface morphology and optical properties parameters after the upper layer deposition were investigated and were correlated with the photocatalytic activity against dye pollution.

## 2. Experimental

The spray pyrolysis method was used to deposit tin sulfide (SnS) thin film on glass substrates at 400 o C using 0.1 M aqueous solutions of Tin chloride (SnCl2.2H2O) and sodium thiosulfate (Na2S2O3.5H2O) obtained at Sigma Aldrich. Each of the two substances was dissolved in 100 ml distilled water and afterward, the mixture was combined to form the final solution. The solution was added another 0.25 ml of concentrated HCl. The deposition of upper SnO2 +CNTs was done by spraying a mixture of 0.1 M SnCl2.2H2O (1 ml) and 0.02 g CNT in 100 ml on the already prepared SnS thin films. Figure 1 presents a plan of the solution preparation steps.

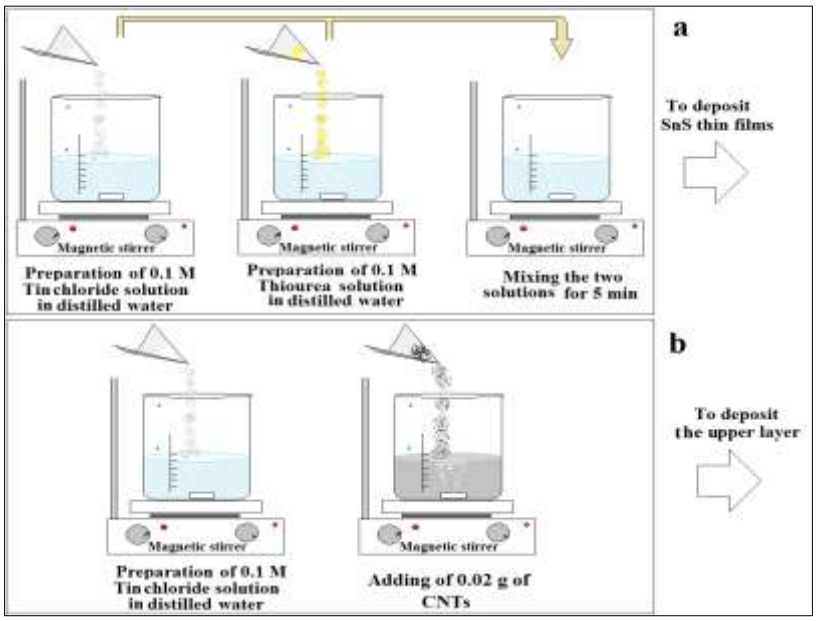


**Figure 1: Steps of solution preparation**

Photocatalytic activity aimed at the degradation of dye pollutants (Methyl blue MW=319.85g/mol) was examined by placing 20 ml of 10 -3 M concentration of synthetic polluted water in a petri dish and rinsed the coated sides in the solution and allowed exposure to the solar radiation of 120 min. The comparisons were made to analyze the pollutant removal efficacy in the contaminated water using the UV-visible spectrometer. Based on Figure 2, the design of a water purification system aimed at the destruction of pollutants via photocatalytic reactions can be achieved by producing a rectangular panel with a diamention of 30.5 18.5 cm2. This design bears 20 glass slides. These slides were formerly coated with the chosen thin films. The total surface area of these slides was close to 375 cm 2. The procedure of experimentation consisted of testing water samples that had been taken in and out of the device that was built. The experiment processes involved injecting the contaminated water into the panel at different low velocities as the slides were subjected to the sunlight.

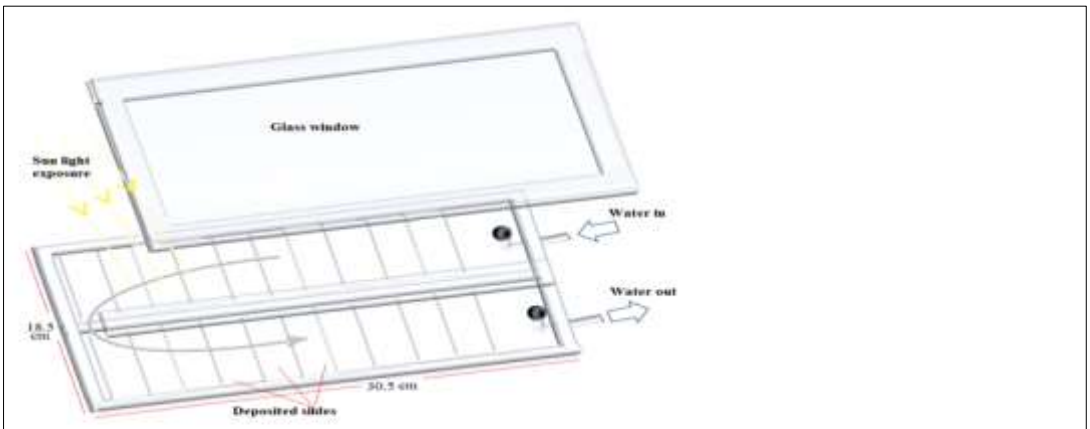


**Figure 2: Schematic representation of the water purification system employing photocatalysis for dye pollutant removal.**

## 3. RESULTS AND DISCUSSIONS

Figure 3 shows a comparison between the XRD patterns of the bare SnS layer and that one coated with the upper layer of SnO2 mixed with carbon nanotube (SnO2:CNT/SnS) synthesized by spray pyrolysis, abbreviated as SCS. Polycrystalline structure is made of the main phase, Zincblende, and another one, Orthorhombic SnS phases, with JCPDF numbers 01-071-3678 and 00-039-0354. The preferable orientation was along the (111) crystallographic plane with a diffraction angle 26.6 o. Orthorhombic and Zincblende phases were also observed in SCS sample but with lower crystallinity compared to bare SnS thin film. Along with this there formed a tetragonal SnO2 phase with (101), (211) and (310) diffraction lines according to JCPDF database No. 96-900-9083, besides a peak at 2 theta = 26.1 degree due to the (002) direction of the carbon nanotubes (CNT) This peak is a characteristic peak due to the c direction of the hexagonal structure which is perpendicular to the radial direction of the CNT. These characters show that the upper layer of SnO2 with the CNTs was successfully deposited. This layer can contribute to the catalytic activity of the surface area by enlarging the surface area and making active sites on the surface. The synthesized movies show a great promise of utilization in different fields due to their unique structural and crystalline properties [14, 15]. The effect of crystallinity exhibited by the upper layer thickness variation offers a good avenue of adjusting the characteristics of such thin films to suit photocatalytic applications [16]. The inter-planar spacing (dhkl) was calculated using Bragg equation and the values of crystallite size (D) were calculated using Scherrer formula as tabulated in Table 1.

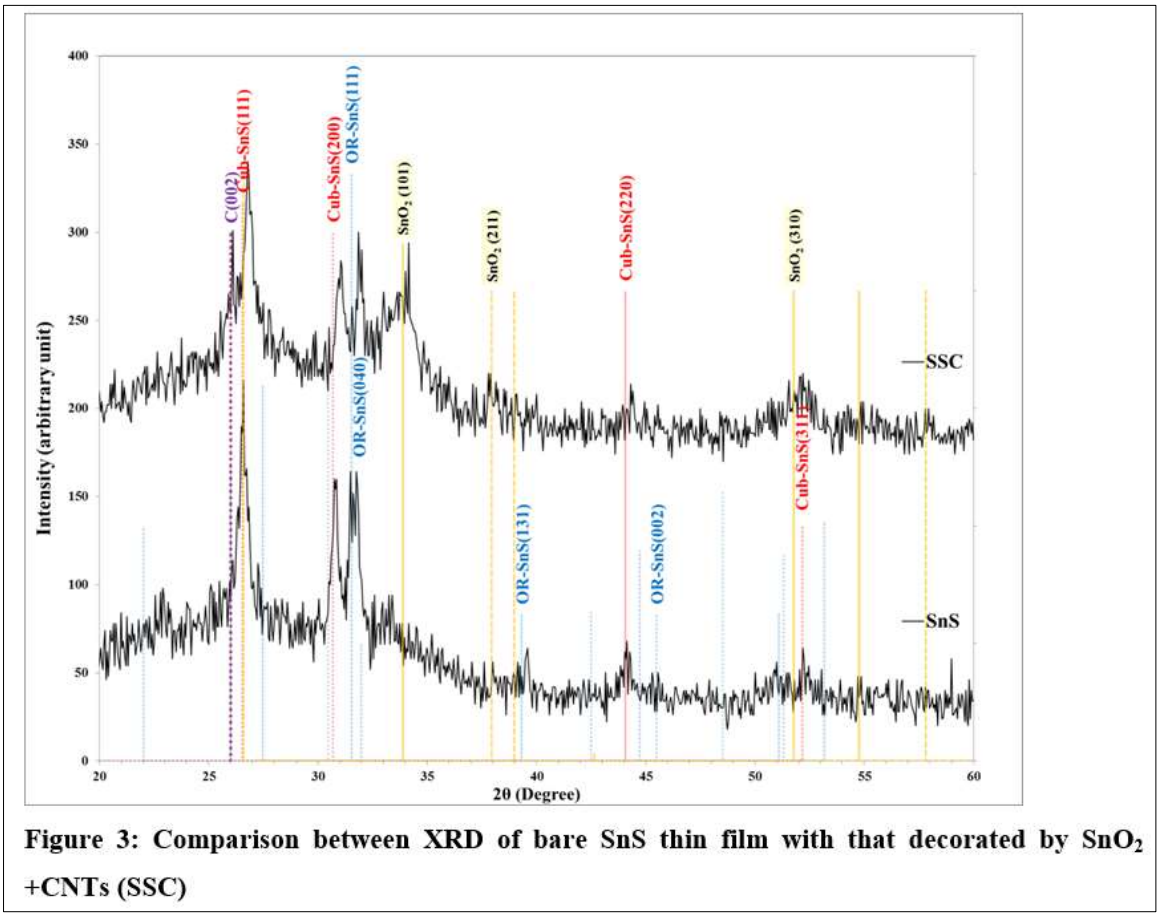


**Figure 3: Comparison between XRD of bare SnS thin film with that decorated by $SnO_2$ +CNTs (SSC)**

The top-view field emission scanning electron microscopy (FE-SEM) images of the deposited SnS and SnO2+CNT/SnS thin films are shown in figure 4 at two different magnifications. SnS sample was in the form of porous nanostructures, which creates high surface area. This porous structure has important implications in photocatalysis, because it presents large spaces where the interactions between the catalyst and target reactants can happen [17]. The sample covered with the upper layer displays a prolonged surface covered with cubic nanostructures of 200 nm edges, which are randomly distributed on the sample surface. These nanostructures can improving the surface activity and the effective area of the surface depending on the sample surface to be used in many applications including photocatalysis.

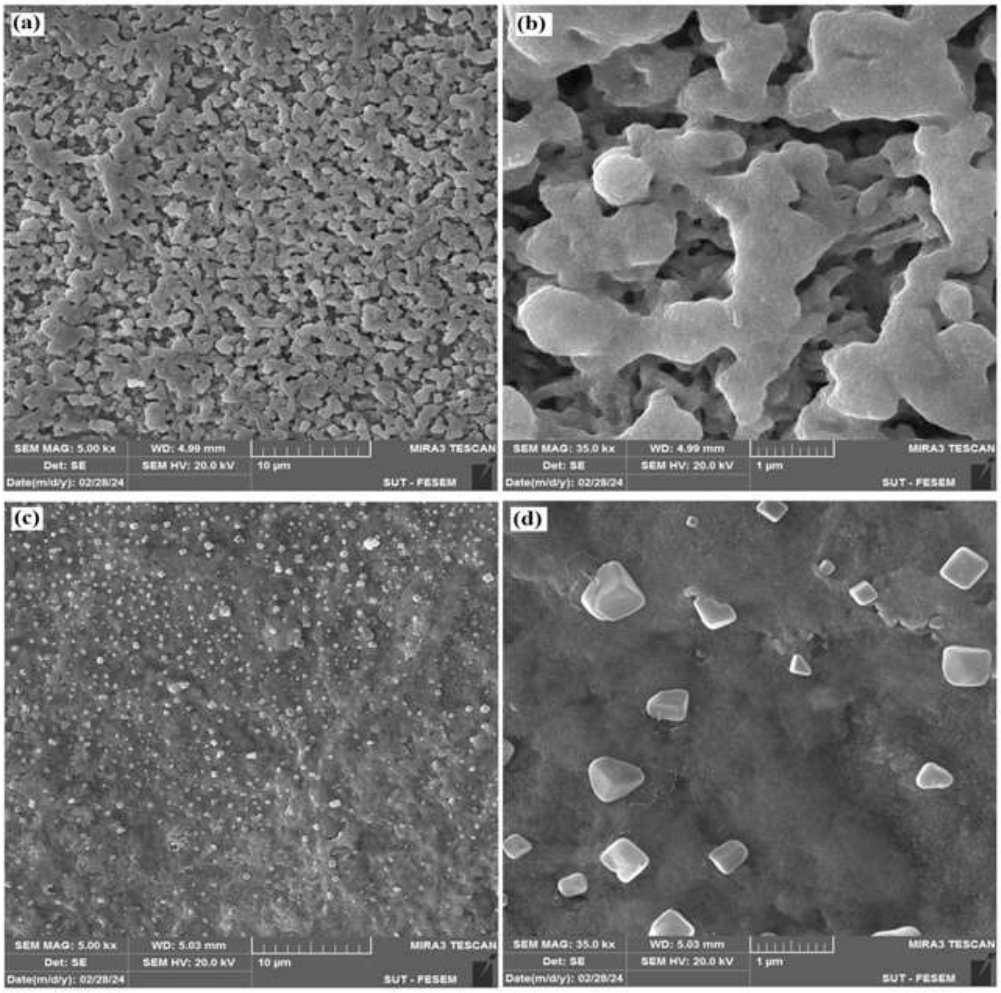


**Figure 4: FE-SEM images at two magnifications of SnS thin film (a and b), coated with $SnO_2$+CNT (c and d).**

Figure 5 shows a comparison of FTIR spectrum of bare SnS thin films and that decorated with SnO2 made with CNT in the wavenumber range of 400 to 4000 cm -1. In the SnS spectrum, absorption bands of 837.9 and 785.4 -1 cm are associated with Sn-S vibration [18]. Other bands at 3404.8 -1 cm -1 OH stretch, 2917.1 and 2846.3 cm -1 CH2 stretch, and 1650.7 cm -1 O-H bend [19], due to adsorbed H2O and carbonyl groups of the ambient were observed. Besides, bands at 1286.2, 1215.4, and 1155.1 cm -1 are associated with the SO2 structure [20]. The decorated sample exhibits identical bands as the SnS, but the additional bands are the SnO2 bands at 612.2 and 523.8 cm -1. There are other bands at 1714.9 cm-1 that is assigned to the C-O stretch. Certain differences are also noticed such as the intensification of the band in proportion to the CH2 motions and the slight displacement of certain bands. The presence of the C-O band, as well as, the intensification of the carbon bans point to the increase of the carbon content in the sample. Such energy change may be assigned to the change in the local atomic structure owing to the strain in the lattice by the local interaction of the upper layer with the SnS surface.

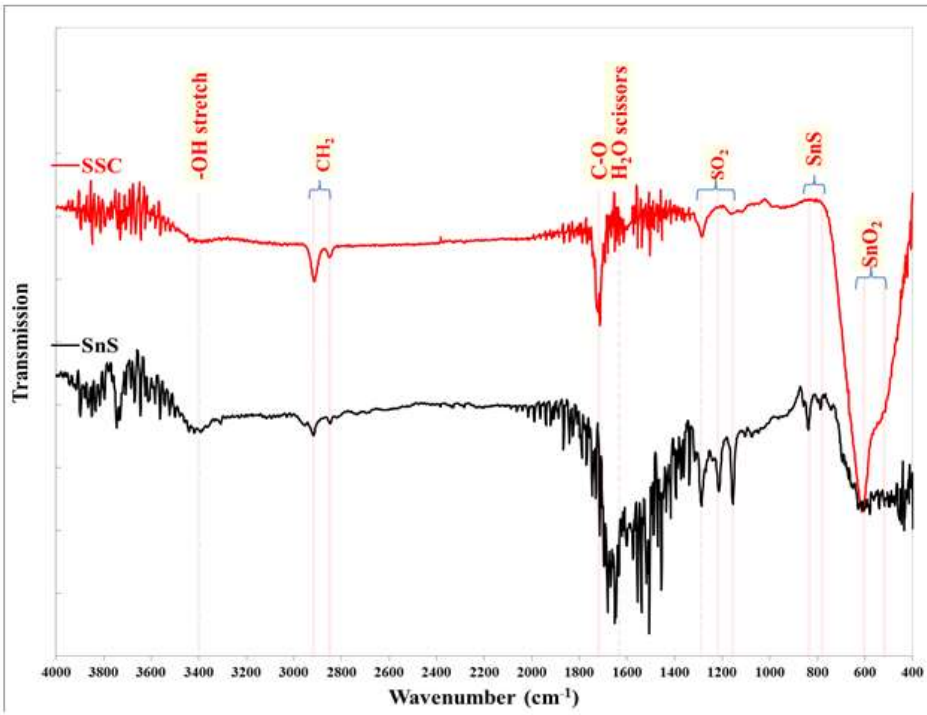


**Figure 5: FTIR patterns of SnS thin film and decorated sample with $SnO_2$+CNT**

**Table 2: FTIR bands of SnS thin film compared with decorated film by $SnO_2$+CNT**

| Band Type | SnS | $SnO_2$+CNT/SnS |
|---|---|---|
| O-H stretch | 3404.9 | 3410.3 |
| $CH_2$ | 2917.1 | 2914.9 |
| | 2846.3 | 2850.1 |
| C-O | - | 1714.9 |
| $H_2O$ | 1650.7 | 1611.7 |
| $SO_2$ | 1286.2 | 1284.5 |
| | 1215.4 | - |
| | 1155.1 | 1154.7 |
| SnS | 837.9 | - |
| | 785.4 | - |
| $SnO_2$ | - | 612.2 |
| | - | 523.8 |

The UV-VIS absorbance spectra and optical energy gap of SnS thin film and that of the one decorated with SnO2+CNT are shown in figure 6. The spectra have a gradually rising absorption edge at about 600 nm. The low degree of crystallinity, i. e. the existence of crystalline defects, is the reason of the non-sharp absorption edge. Absorption highly enhanced by coating with the top layers of SnO2+CNT. The increase in absorbance implies the same in photo applications of enhancing the ability to absorb visible light and therefore improve the ability to harvest solar energy. Optical energy gap enhancing was observed after the deposition of upper layers of SnO2 +CNT which increased form 2eV to 2.4.

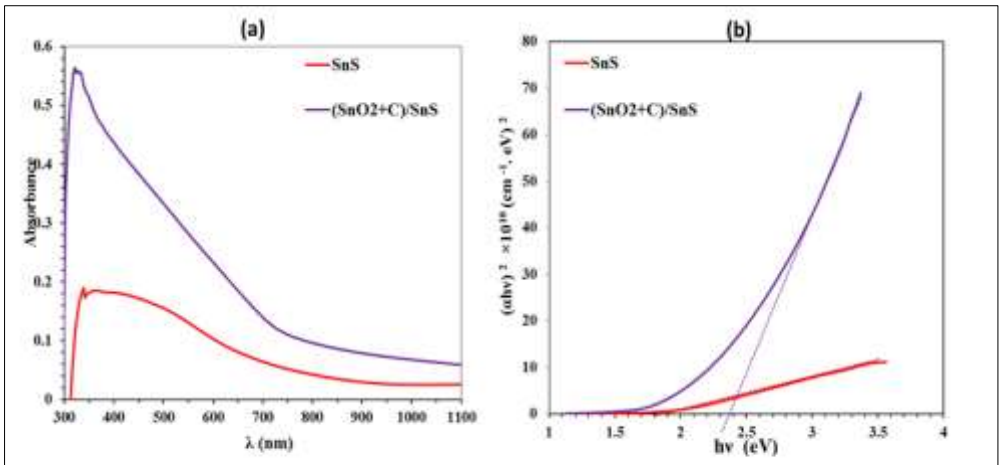


**Figure 6: UV-visible absorbance (a) and Tauc plot (b) of SnS thin film decorated with $SnO_2$ +CNT**

The synthesized spray-formed thin films were characterized with regard to photocatalytic use against a synthetic solution of Methyl blue (MB). The normalization of the synthetic solution of the dye at various concentrations is exhibited in figure (7). The UV-visible absorbance displaying the highest absorbance at approximately 665 nm wavelength is dependent on the concentration of dye in a solution. The fitting curve of the maximum absorbance values versus the solution concentration was obtained as presented in figure (5-b) based on the equation.

**Concentration = 2.084 10-7 e5.641 Abs. [R 2 =0.9999] …….(1)**

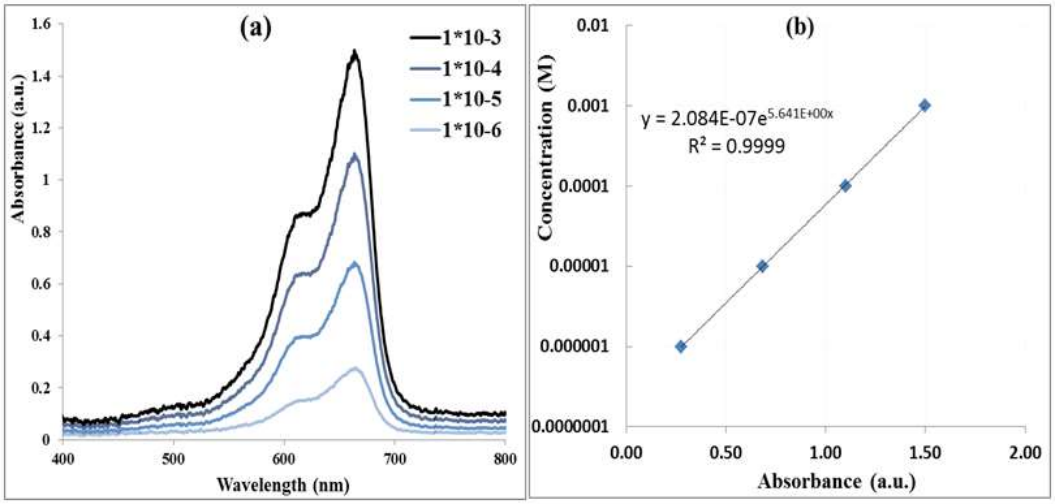


**Figure 7: Normalization process for absorbance of Methyl blue absorbance in solutions at different concentrations.**

When testing the photocatalytic activity with the help of methyl blue as a dye, it is usually important to control the conditions (environment) in which the degradation takes place by means of pH adjustment. The variation of the pH allows investigating the photocatalytic activity under varied conditions, which can be crucial in the water treatment due to dye contamination. The photocatalytic efficiency is usually followed by the decrease in the absorbance of the methyl blue degradation.

The absorbance spectra of the MB dye solutions in varying pH in the presence of bare SnS and decorated thin film samples before and after 120 min solar exposure are depicted in figure (8). A distinct reduction in the maximum absorbance at various rates based on the photocatalytic activity of the sample was observed when the dye solution was placed in the position perpendicular to the samples exposed directly to the solar radiation (at 90). The concentration of dyes was calculated using the normalization equation. The efficiency of degradation was determined based on the equation.

$$\text{Degradation efficincy} = (1 - \frac{C_t}{C_0}) \times 100\%$$

$C_o$ is the initial concentration of the dye and $C_t$ is the concentration of the dye at the desired time (120 min).

Higher degradation efficiency in one of the samples compared to the other was explained by the difference in the energy band gaps and the surface properties of the samples (Table 3). The 2.4 eV (effective wavelength 516 nm) band gap, corresponding approximately to the maximum of the solar spectrum, can generate highly reactive oxidative species, capable of more effectively degrading the organic dyes. On the other hand, the maximum degradation efficiency was observed on the primary side at 8 pH in contrast to neutral or acidic solutions. The bare SnS sample and that coated with the upper layer suffered the maximum degradation of 89.74% and 95.84%, respectively, after an exposure time of 120 min. The top electrode of the various conductive kinds can form junctions, which modify the electronic properties, and generate active sites, which respond with the pollutant molecules.

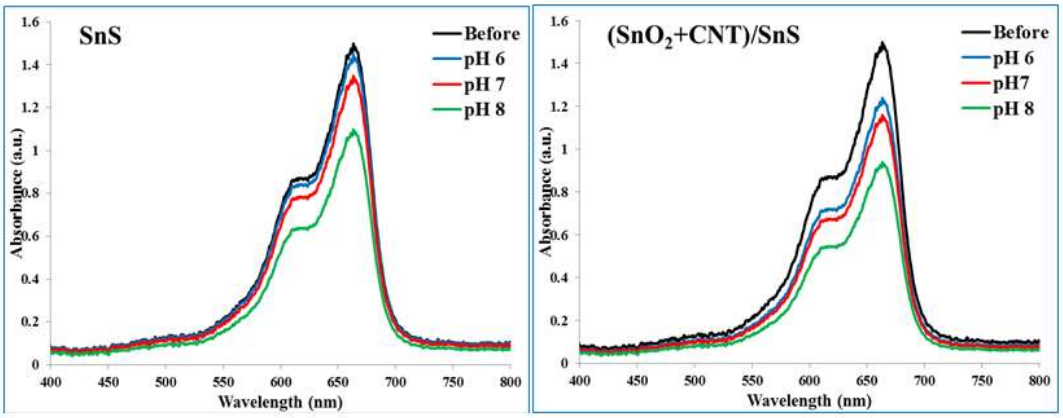


**Figure 8: absorbance spectra of MB dye solutions at different pH before and after 120 min solar exposure with SnS thin film (a) and decorated samples (b).**

**Table 3: Max absorbance and calculated degradation efficiency of dye solutions at different pH after 120 min solar exposure with the aid of the coated samples.**

| Sample | pH | Abs | Conc. (M) | Degradation (%) |
|---|---|---|---|---|
| SnS | 6 | 1.45 | 7.4E-04 | 26.27% |
| | 7 | 1.35 | 4.2E-04 | 58.03% |
| | 8 | 1.10 | 1.0E-04 | 89.74% |
| $(SnO_2+CNT)/SnS$ | 6 | 1.24 | 2.3E-04 | 77.42% |
| | 7 | 1.16 | 1.4E-04 | 85.62% |
| | 8 | 0.94 | 4.2E-05 | 95.84% |

Sample (SnO2+CNT)/SnS was chosen to be studied with four water samples in the model system design. Analysis of water quality was carried out using different tests to determine the water quality before and after treatment. There are aquatic life and human health limitation levels of each test. Table 4 indicates the water quality parameters of the four water samples of the various locations of Al-Hilla River in Iraq on 1/12/2025 before and after entering the system design work based on the principle of photocatalysis. The findings were compared to the conventional limitation values of the water quality parameter, since WHO suggested it to the aquatic life and human consumption. The system was modified to 1L/h flow rate.

The alkalinity (pH) incorporates the neutralization of water. Either low or high alkalinity may cause damages to aquatic life. Such stability means that the neutrality of the water is well maintained by the photocatalytic system without any considerable fluctuations. As illustrated in the table, the values fall within the WHO standard, hence the water is of human consumption quality and will not harm aquatic life. All the samples lose their electrical conductivity (EC) due to the treatment. Such a decrease shows that the concentration of ions decreases as a result of either the absorption of ions or deposition of certain compounds on the nanoparticle surface. The EC values are below the WHO limit and this indicates improved water quality. As an illustration, in Sample A, TDS decreases to 249.5 mg/L, which is way below the WHO maximum of 1500 mg/L. This decrease shows that the system is efficient in removing dissolved matter such as organic compounds. The organic compounds may be of natural origin or may be farm or industrial effluents. Their elimination is

essential to the enhancement of water quality, taste, and safety. Low TDS also guarantees lesser scaling and fouling in water distribution system. This means that the treated water is more palatable to human beings.

There is a slight reduction in the values of turbidity (TUR) of the treated water. As an example, Sample A decreases 6.1 to 4.5 NTU. These values are within the WHO standard of 5 NTU, which guarantees greater clarity and less polluted water. Each ion ($Ca^{2+}$, Na +, K +, Cl, NO 3, SO 4 2, PO 4 3 ) is reduced by a small margin and is well below the WHO limit, which increases safety and reduces risk in the water environment. Metal sulfide nanoparticles can adsorb part of the components found in water, including ions or organic matter. This process may alter the composition of water and, therefore, its chemical characteristics. The dissolved oxygen (DO) of water was (slightly) upgraded after the water treatment by the photocatalysis process owing to the production of oxygen during the photocatalytic reactions. Photocatalysis is the use of a photocatalyst excited by light, which is capable of producing reactive oxygen species (ROS) hydroxyl radicals (OH) and superoxide anions (O2−). These reactions could facilitate the dissolution of atmospheric oxygen or they could produce molecular oxygen at the site. This enhances the oxygenation of the water and hence the overall quality of water and it may render it more acceptable to the aquatic fauna and other uses of the environment. These shifts indicate the ability of the photocatalytic system to significantly remove organic pollutants, marginally lower the minerals concentration and improve the dissolved oxygen.

**Table 4: values of water quality tests before and after treatment of sample the three selected water samples compared with the WHO standard**

| Par. | A | | B | | C | | D | | WHO Standards (mg/L) |
|---|---|---|---|---|---|---|---|---|---|
| | Before | After | Before | After | Before | After | Before | After | |
| pH | 7.9 | 7.1 | 7.15 | 7.2 | 7.8 | 7.1 | 8.1 | 7.1 | 6.5–8.5 |
| $DO_2$ | 7.5 | 8.5 | 7.7 | 8.7 | 7.6 | 8.6 | 7.7 | 8.7 | >4 mg/L |
| $NO_3^-$ | 4.21 | 3.1 | 4.1 | 3.1 | 5 | 3.5 | 5.3 | 3.9 | 50 |
| $PO_4^{3-}$ | 0.2 | 0.18 | 0.2 | 0.17 | 0.29 | 0.26 | 0.33 | 0.32 | 0.57 |
| K+ | 4.7 | 4.5 | 4.1 | 3.8 | 5.1 | 4.6 | 5.5 | 5.1 | 40 |
| $Mg^{+2}$ | 46 | 44.2 | 34.9 | 34.4 | 35.6 | 37.8 | 39.4 | 38.8 | 50 |
| $Ca^{2+}$ | 117 | 91.7 | 121.7 | 93.8 | 153 | 109.6 | 1.55 | 1.2 | 200 |
| $Na^+$ | 24.9 | 18.4 | 86.3 | 68.3 | 85.2 | 62.2 | 80.2 | 63.8 | 200 |
| $SO4^{2-}$ | 367.2 | 310.1 | 326 | 260.5 | 399 | 321.2 | 420.2 | 314.4 | 400 |
| $Cl^-$ | 150 | 131.9 | 155.7 | 133.7 | 160.2 | 131.4 | 166.2 | 131.4 | 600 |
| TDS | 744.6 | 249.5 | 766.9 | 257.1 | 840 | 320.1 | 877 | 320.1 | 1500 |
| EC | 1200 | 1098.5 | 1237 | 1218.1 | 1286 | 1174.9 | 1298 | 1249.5 | 2300 |
| TUR | 1.62 | 1.2 | 2 | 1.5 | 5.8 | 4.6 | 6.6 | 4.9 | 5 |

## 4. CONCLUSIONS

In this work, an easy and inexpensive method was used to fabricate one layer of SnS thin film and two-layered SnO2+CNTs/SnS thin. XRD analysis applied to ascertain the nanocrystalline nature of the two samples of mixed phases of the extra phases that matched the upper layer of SnO2 mixed with the carbon tubes. The porous framework of SnS and other attached cubic nano structures were revealed by FE-SEM, when the upper layer was deposited. As the FTIR result shows, there are addition bands at the SnO2 and strengthening bands intensities at the carbon bands. The UV-visible spectroscopy proved the enhanced absorbance that enhances the solar radiation harvesting and variation in the optical bandgap with deposition of the upper layer to 2.4 eV that is optimum solar spectrum. The results point toward the possibility of customizing structural and optical characteristics through the creation of the heterojunctions. Heterojunctions between SnS and SnO2 can also be formed, which would assist in charge separation and enhance the reactivity of the site. Moreover, the surface area of the sample can be increased by the added CNTs. The deposition of the upper layer results in the synergy of the many points and increase of the photocatalytic activity of the MB solution. This band gap was 2.4 eV, which is approximately at the maximum of the solar spectrum and the difference in the surface behavior led to the more effective breakdown of the organic dyes. Also, the maximum degradation efficiency was observed at slightly primary at 8 pH. This

nanocomposits structure that is formed has a great potential in enhancing water treatment by effectively removing the dye besides other pollutants reductions.

## REFERENCES


1. R.M. Navarro, F. del Valle, J.A. Villoria de la Mano, M.C. Álvarez-Galván, J.L.G. Fierro, Photocatalytic Water Splitting Under Visible Light: Concept and Catalysts Development, Adv. Chem. Eng. 36 (2009) 111–143. https://doi.org/10.1016/S0065-2377(09)00404-9.
2. A. Abdel Aal, S.A. Mahmoud, A.K. Aboul-Gheit, Sol-gel and thermally evaporated nanostructured thin ZnO films for photocatalytic degradation of trichlorophenol, Nanoscale Res. Lett. 4 (2009) 627–634. https://doi.org/10.1007/S11671-009-9290-1/FIGURES/11.
3. S. Navarro, J. Fenoll, N. Vela, E. Ruiz, G. Navarro, Photocatalytic degradation of eight pesticides in leaching water by use of ZnO under natural sunlight, J. Hazard. Mater. 172 (2009) 1303–1310. https://doi.org/10.1016/J.JHAZMAT.2009.07.137.
4. A.A. Meshram, K. Aashish Moses, S.S. Baral, S.M. Sontakke, Hydrogen production from water splitting of real-time industry effluent using novel photocatalyst, Adv. Powder Technol. 33 (2022) 103488. https://doi.org/https://doi.org/10.1016/j.apt.2022.103488.
5. T. Mohammad, F. Alam, A. Sadhanala, H.M. Upadhyaya, V. Dutta, Tin Sulfide (SnS) Films Deposited by an Electric Field-Assisted Continuous Spray Pyrolysis Technique with Application as Counter Electrodes in Dye-Sensitized Solar Cells, ACS Omega. 7 (2022) 39690–39696. https://doi.org/10.1021/acsomega.2c03454.
6. C. Gao, H. Shen, L. Sun, Preparation and properties of zinc blende and orthorhombic SnS films by chemical bath deposition, Appl. Surf. Sci. 257 (2011) 6750–6755. https://doi.org/10.1016/j.apsusc.2011.02.116.
7. N. Aparna, R.S. Philip, M. Mathew, Photocatalytic activities of SnS thin films deposited at room temperature, Appl. Surf. Sci. Adv. 13 (2023) 100374. https://doi.org/10.1016/j.apsadv.2023.100374.
8. S.A. Patil, H.T. Bui, S. Hussain, I. Rabani, Y. Seo, J. Jung, N.K. Shrestha, H. Kim, H. Im, Self-standing SnS nanosheet array: a bifunctional binder-free thin film catalyst for electrochemical hydrogen generation and wastewater treatment, Dalt. Trans. 50 (2021) 12723–12729. https://doi.org/10.1039/D1DT01855H.
9. S.A. Patil, N.K. Shrestha, S. Hussain, J. Jung, S.-W. Lee, C. Bathula, A.N. Kadam, H. Im, H. Kim, Catalytic decontamination of organic/inorganic pollutants in water and green H2 generation using nanoporous SnS2 micro-flower structured film, J. Hazard. Mater. 417 (2021) 126105. https://doi.org/10.1016/j.jhazmat.2021.126105.
10. R.A. Rani, A.S. Zoolfakar, A.P. O'Mullane, M.W. Austin, K. Kalantar-Zadeh, Thin films and nanostructures of niobium pentoxide: fundamental properties, synthesis methods and applications, J. Mater. Chem. A. 2 (2014) 15683–15703. https://doi.org/10.1039/C4TA02561J.
11. J.E. Hill, R.R. Chamberlin, Process for making conductive film, (1964).
12. S. Pigeot-Rémy, F. Simonet, E. Errazuriz-Cerda, J.C. Lazzaroni, D. Atlan, C. Guillard, Photocatalysis and disinfection of water: Identification of potential bacterial targets, Appl. Catal. B Environ. 104 (2011) 390–398. https://doi.org/10.1016/J.APCATB.2011.03.001.
13. R.A. Damodar, S.J. You, H.H. Chou, Study the self cleaning, antibacterial and photocatalytic properties of TiO2 entrapped PVDF membranes, J. Hazard. Mater. 172 (2009) 1321–1328. https://doi.org/10.1016/J.JHAZMAT.2009.07.139.
14. P.C. Huang, J.L. Huang, S.C. Wang, M.O. Shaikh, C.Y. Lin, Photoelectrochemical properties of orthorhombic and metastable phase SnS nanocrystals synthesized by a facile colloidal method, Thin Solid Films. 596 (2015) 135–139. https://doi.org/10.1016/j.tsf.2015.09.081.
15. L.A. Burton, A. Walsh, Phase Stability of the Earth-Abundant Tin Sul fi des SnS, SnS2 , and Sn2S3, J. Phys. Chem. C. 116 (2012) 24262−24267.
16. L. Dashairya, M. Sharma, S. Basu, P. Saha, SnS2/RGO based nanocomposite for efficient photocatalytic degradation of toxic industrial dyes under visible-light irradiation, J. Alloys Compd. 774 (2018) 625–636. https://doi.org/10.1016/j.jallcom.2018.10.008.
17. A. Taufik, R. Saleh, G. Seong, Enhanced photocatalytic performance of SnS2 under visible light irradiation: strategies and future perspectives, Nanoscale. (2024) 1–15. https://doi.org/10.1039/d4nr00706a.
18. J. Srivind, S. Balamurugan, K. Usharani, D. Prabha, M. Suganya, V.S. Nagarethinam, A.R. Balu, Visible light irradiated photocatalytic and magnetic properties of Fe-doped SnS2 nanopowders, J. Mater. Sci. Mater. Electron. 29 (2018) 9016–9024. https://doi.org/10.1007/s10854-018-8926-2.
19. H. Hajifatheali, E. Ahmadi, A. Wojtczak, Z. Jaglicic, The synthesis of N-methylbis[2-(dodecylthio)ethyl]amine (SNS) and investigation of its efficiency as new mononuclear catalyst complex in copper-based ATRP, Macromol. Res. 23 (2015) 977–985. https://doi.org/10.1007/s13233-015-3132-z.
20. O.G. Buzykin, S. V. Ivanov, A.A. Ionin, A.A. Kotkov, A.Y. Kozlov, Spectroscopic detection of sulfur oxides in the aircraft wake, J. Russ. Laser Res. 26 (2005) 402–426. https://doi.org/10.1007/s10946-005-0043-z.